Available online at www.sciencedirect.com
ScienceDirect
Mathematics and Computers in Simulation 215 (2024) 543–559
MATHEMATICS AND COMPUTERS IN SIMULATION
www.elsevier.com/locate/matcom

Original articles

A high-order multi-resolution wavelet method for nonlinear systems of differential equations

Muhammad Ahsan[a,b,*], Weidong Lei[b], Martin Bohner[c], Amir Ali Khan[a]

[a] *Department of Mathematics, University of Swabi, Khyber Pakhtunkhwa 23200, Pakistan*
[b] *School of Civil and Environmental Engineering, Harbin Institute of Technology, Shenzhen, 518055, China*
[c] *Department of Mathematics and Statistics, Missouri S&T, Rolla, MO 65409-0020, USA*

Received 8 December 2022; received in revised form 15 July 2023; accepted 21 August 2023
Available online 26 August 2023

Abstract

In this article, the applications of the new Haar wavelet collocation methods called as Haar wavelet collocation method (HWCM) and higher-order Haar wavelet collocation method (H-HWCM) are developed for the solution of linear and nonlinear systems of ordinary differential equations. The proposed H-HWCM is compared with a variety of other methods including the well-known HWCM. The quasi-linearization technique is introduced in the nonlinear cases. The stability and convergence of both techniques is studied in detail, which are the important parts to analyze the proposed methods. The efficiency of the methods is illustrated with certain numerical examples, but the H-HWCM is more accurate with faster convergence than the HWCM and other methods reported in the literature.

Keywords: Haar wavelet; H-HWCM; System of nonlinear differential equations; Collocation method; Quasi-linearization technique

1. Introduction

Differential equations are widely recognized as the foundation for physical systems. In engineering, population dynamics, applied mathematics, physics, economics, astronomy, and other related subjects, ordinary differential equations (ODEs) and partial differential equations (PDEs) are suited to describe a wide range of phenomena [17,23,39,42,43,47]. To find analytical solutions of nonlinear differential equations is challenging in most circumstances due to the existence of nonlinear terms, and therefore an alternate procedure is compulsory to deal with them. To solve alternatively these nonlinear equations, different numerical methods have been widely used such as the predictor–corrector technique [14], Runge–Kutta method [51], and a finite element approach [45]. These numerical approaches demand that the domain be discretized into a finite number of points.

The growth or decay of bacteria, half-life of a radioactive substance, age of a fossils, Newton's law of cooling and warming, mixture of two salt solutions, and different types of series circuits can be represented by ODEs [53].

* Corresponding author.
E-mail address: ahsankog@uos.edu.pk (M. Ahsan).

https://doi.org/10.1016/j.matcom.2023.08.032

Similarly, systems of ODEs are also employed in a variety of scientific and engineering sectors. Observing the mixing problem involving two tanks, electrical networks, and mass–spring systems can be represented by a system of ODEs [25]. In the same manner, population models of different spaces, the logistic equation, rate of chemical reactions, and competition models like Lotka–Volterra predator–prey models are better explained by nonlinear systems of ODEs [53].

Systems of ODEs have also been solved using proper numerical techniques. The differential transform approximation [26], Haar wavelets collocation methods [10,21], Adomian decomposition method [12], artificial neural networks technique [27], and Legendre neural network method [37] are some of the available techniques to solve linear and nonlinear system of ODEs.

Among wavelets, the simplest ones are Haar wavelets, which are described by piecewise continuous functions. Haar wavelets are observed as extremely effective tools to calculate solutions of ODEs and PDEs, and they have been applied to solve a variety of problems in biology, physics, fluid dynamics, and chemical reactions. Chen and Hsiao were the first to develop the Haar wavelet approach and executed it on differential equations to get the required solution [13,20]. Hariharan also developed the Haar wavelet technique for solving the Klein–Gordon problem and the sine–Gordon equation [18]. He also presented an accurate and economical Haar wavelet technique to solve the well-known Cahn–Allen problem [19] and Fisher's equation [19]. Aziz et al. [11] presented a new numerical technique for solving nonlinear integral-type equations with the help of Haar wavelets. Ahsan et al. further extended the Haar wavelet approach to solve linear and nonlinear direct problems [1,9,30,31] and inverse problems [4,6,7,48]. Apart from these, several other researchers have exploited Haar wavelets as a problem-solving tool in their respective fields of interest [8,22,28,34,35]. The most sophisticated use of Haar wavelets is demonstrated in [41] for the identification of software piracy levels. Apart from the wavelet collocations methods, other mesh based and meshless methods have also been developed to solve linear and nonlinear ODEs, PDEs and fractional differential equations [2,15,16,46].

All of the previous studies have followed the Chen and Hsiao approach [13], where the highest order derivatives present in the model equation (such as $\frac{d^n y}{dx^n}$) is approximated by Haar series. In 2018, Majak et al. developed a high-order Haar wavelet collocation method (H-HWCM) [32] by modifying the Chen and Hsiao approach [13] to solve ODEs. According to H-HWCM the $\frac{d^{n+2s} y}{dx^{n+2s}}$ (where $s = 1, 2, \dots$) is approximated by Haar series instead of $\frac{d^n y}{dx^n}$ term. The H-HWCM is recently applied to solve ODEs [3,33], nonlinear evolution equations [44], and nonlinear PDEs [52]. The H-HWCM is also used to study the static response and buckling loads of multilayered composite beams [49] and vibration analysis of different types of beams [36,38,40]. Furthermore, the H-HWCM is recently implemented to solve nonlinear problems with two point-integral boundary conditions [5].

In this paper, we extend the H-HWCM to solve the system of nonlinear ordinary differential equations (NLODEs)

$$\begin{aligned} \frac{\mathrm{d}y_1}{\mathrm{d}x} &= \mathfrak{F}_1(x, y_1, y_2, \dots, y_n), \\ \frac{\mathrm{d}y_2}{\mathrm{d}x} &= \mathfrak{F}_2(x, y_1, y_2, \dots, y_n), \\ &\vdots \\ \frac{\mathrm{d}y_n}{\mathrm{d}x} &= \mathfrak{F}_n(x, y_1, y_2, \dots, y_n), \end{aligned} \tag{1}$$

subject to the set of initial conditions

$$\{y_1(0), y_2(0), \dots, y_n(0)\} = \{\alpha_1, \alpha_2, \dots, \alpha_n\}, \tag{2}$$

where $\mathfrak{F}_p$ and α_p, $p = 1, 2, \dots, n$, are nonlinear functions and real constants, respectively. This type of stiff problems has applications in nonlinear mechanics, chemical engineering, biochemistry, etc. Unfortunately, analytical solutions to this type of stiff systems do not exist, so that numerical solutions are an alternate option to deal with them.

In this article, the study presented in [3,32] has been extended to solve NLODEs. The iterative quasi-linearization technique is used to linearize NLODE and H-HWCM, and it is then implemented to get the numerical solution.

2. Haar functions

A generalized representation of the Haar functions is defined as

$$h_i(x) = \begin{cases} 1 & \text{for} \quad x \in [\beta_1(i), \beta_2(i)), \\ -1 & \text{for} \quad x \in [\beta_2(i), \beta_3(i)), \\ 0 & \text{elsewhere}, \end{cases} \tag{3}$$

where

$$\begin{cases} \beta_1(i) = A + \dfrac{(B-A)k}{m}, \quad \beta_2(i) = A + \dfrac{(B-A)(k+0.5)}{m}, \quad \beta_3(i) = A + \dfrac{(B-A)(k+1)}{m}, \\ i = m + k + 1, \quad k = 0, 1, \ldots, m-1, \quad m = 2^j, \quad j \in \mathbb{N}_0. \end{cases} \tag{4}$$

The component of the wavelet is represented by m, whereas the translation parameter is described by k. It is to be noticed that $i \geq 2$, so we define the mother wavelet by

$$h_1(x) = \begin{cases} 1 & \text{for} \quad x \in [A, B], \\ 0 & \text{elsewhere}. \end{cases}$$

The notation $p_{i,n}(x)$ indicates the nth-order integrals of the Haar functions, where $i \in \mathbb{N}$, and can be obtained by analytical calculation to keep the derivations simple, namely

$$p_{i,n}(x) = \begin{cases} 0 & \text{for} \quad x < \beta_1(i), \\ \frac{1}{n!}\Big(x - \beta_1(i)\Big)^n & \text{for} \quad x \in [\beta_1(i), \beta_2(i)), \\ \frac{1}{n!}\Big((x-\beta_1(i))^n - 2(x-\beta_2(i))^n\Big) & \text{for} \quad x \in [\beta_2(i), \beta_3(i)), \\ \frac{1}{n!}\Big((x-\beta_1(i))^n - 2(x-\beta_2(i))^n + (x-\beta_3(i))^n\Big) & \text{for} \quad x \geq \beta_3(i), \end{cases}$$

and

$$p_{1,n}(x) = \frac{(x-A)^n}{n!}.$$

3. Numerical methods

We will approximate the solution of a system of differential equations by two methods.

3.1. Haar wavelet collocation method (HWCM)

Several Haar wavelet collocation methods (HWCMs) are used for solving a system of differential equations following the Chen and Hsiao method [13]. In this method, we approximate the derivative of the highest-order in the ODE by Haar series. For example, if we solve the system (1), then we approximate

$$\begin{aligned} \frac{\mathrm{d}y_1}{\mathrm{d}x} &= \sum_{i=1}^{2M} a_i^{(1)} h_i(x), \\ \frac{\mathrm{d}y_2}{\mathrm{d}x} &= \sum_{i=1}^{2M} a_i^{(2)} h_i(x), \\ &\vdots \\ \frac{\mathrm{d}y_n}{\mathrm{d}x} &= \sum_{i=1}^{2M} a_i^{(n)} h_i(x), \end{aligned} \tag{5}$$

where $a_i^{(p)}$, $p = 1, 2, \ldots, n$, are the unknown Haar wavelet coefficients. The approximate solutions $y_1, y_2, \ldots, y_n$, can be obtained by integrating (5), such as

$$\begin{aligned} y_1(x) &= \sum_{i=1}^{2M} a_i^{(1)} p_{i,1}(x) + k_1, \\ y_2(x) &= \sum_{i=1}^{2M} a_i^{(2)} p_{i,1}(x) + k_2, \\ &\vdots \\ y_n(x) &= \sum_{i=1}^{2M} a_i^{(n)} p_{i,1}(x) + k_n, \end{aligned} \tag{6}$$

where $k_1, k_2 \ldots, k_n$ are the constants of integration. The nonlinear system of Eqs. (1) can be linearized using the following auxiliary result.

Lemma 1. *Let ℓ_1 and ℓ_2 be two C^1 functions defined on $[A, B]$. For $p^* = 1, 2, \ldots, P^*$*

$$\ell_1^{p^*+1}(x)\ell_2^{p^*+1}(x) = \ell_1^{p^*+1}(x)\ell_2^{p^*}(x) + \ell_1^{p^*}(x)\ell_2^{p^*+1}(x) - \ell_1^{p^*}(x)\ell_2^{p^*}(x) + \mathcal{O}(\Delta x)^2,$$

where $\Delta x = \frac{B-A}{2M}$, and p^* represents the iteration number.

Proof. See [4] and the references therein. □

After linearization of (1), (5) and (6) are utilized with the collocation points

$$x_j = a + \frac{(b-a)(j-0.5)}{2M}.$$

This process converts the system of ODEs into $2M$ algebraic equations with $2M + n$ unknowns. The other n equations can be achieved by introducing the given n initial conditions (2) in (6). Hence, solving the $2M + n$ algebraic equations for $2M + n$ unknowns and then putting these Haar coefficients along with integration constants back in the expression $y_1(x)$, $y_2(x), \ldots, y_n(x)$, the required approximate solution can be obtained. The numerical solution at any point $x_{k^*} \in [A, B]$ can also be acquired by the interpolation formula

$$\begin{aligned} y_1(x_{k^*}) &\approx \sum_{i=1}^{2M} a_i^{(1)} p_{i,1}(x_{k^*}) + k_1, \\ y_2(x_{k^*}) &\approx \sum_{i=1}^{2M} a_i^{(2)} p_{i,1}(x_{k^*}) + k_2, \\ &\vdots \\ y_n(x_{k^*}) &\approx \sum_{i=1}^{2M} a_i^{(n)} p_{i,1}(x_{k^*}) + k_n. \end{aligned} \tag{7}$$

3.2. H-HWCM

Fast convergent wavelet methods are used for solving differential equations following H-HWCM [32]. In H-HWCM, instead of approximating the highest-order derivative present in the model equation, we start with the approximation

$$\begin{aligned} \frac{\mathrm{d}^{(1+2s)} y_1}{\mathrm{d}x^{(1+2s)}} &= \sum_{i=1}^{2M} a_i^{(1)} h_i(x), \\ \frac{\mathrm{d}^{(1+2s)} y_2}{\mathrm{d}x^{(1+2s)}} &= \sum_{i=1}^{2M} a_i^{(2)} h_i(x), \end{aligned}$$

$$\vdots$$
$$\frac{\mathrm{d}^{(1+2s)}y_n}{\mathrm{d}x^{(1+2s)}} = \sum_{i=1}^{2M} a_i^{(n)} h_i(x), \tag{8}$$

where $s = 1, 2, \ldots$. Integrating (8) $1+2s$ times, we get

$$\begin{aligned} y_1(x) &= \sum_{i=1}^{2M} a_i^{(1)} p_{i,1+2s}(x) + \sum_{r=0}^{2s} c_r^{(1)} \frac{x^r}{r!}, \\ y_2(x) &= \sum_{i=1}^{2M} a_i^{(2)} p_{i,1+2s}(x) + \sum_{r=0}^{2s} c_r^{(2)} \frac{x^r}{r!}, \\ &\vdots \\ y_n(x) &= \sum_{i=1}^{2M} a_i^{(n)} p_{i,1+2s}(x) + \sum_{r=0}^{2s} c_r^{(n)} \frac{x^r}{r!}, \end{aligned} \tag{9}$$

where $c_0^{(p)}, c_1^{(p)}, \ldots, c_{2s}^{(p)}$, $p = 1, 2, \ldots, n$, are integration constants. Following Lemma 1, we can linearize (1). Then using (8) and (9) with the collocation points $x_j = a + \frac{(b-a)(j-0.5)}{2M}$ in the linearized equation, we get $2M$ algebraic equations in $2M + n(1+2s)$ unknowns. The n equations (for $c_0^{(p)}$, $p = 1, 2, \ldots, n$) can be obtained by introducing the given n initial conditions in (9), while the remaining $n \times 2s$ equations (for $c_1^{(p)}, \ldots, c_{2s}^{(p)}$, $p = 1, 2, \ldots, n$) can be obtained by introducing the nodal points other than the collocation points into the linearized Haar wavelet expression of the (1), namely

$$x_l = a + \frac{l}{2M}, \qquad x_\ell = b - \frac{\ell}{2M}, \qquad l = \ell = 0, 1, \ldots, s-1. \tag{10}$$

After finding all the Haar coefficients along with integration constants and then putting these values back in the expression in (9) $(y_1(x),\ y_2(x), \ldots, y_n(x))$, the required approximate solution can be obtained. The numerical solution at any point $x_{k^*} \in [A, B]$ can also be acquired by the interpolation formula

$$\begin{aligned} y_1(x_{k^*}) &\approx \sum_{i=1}^{2M} a_i^{(1)} p_{i,1+2s}(x_{k^*}) + \sum_{r=0}^{2s} c_r^{(1)} \frac{x_{k^*}^r}{r!}, \\ y_2(x_{k^*}) &\approx \sum_{i=1}^{2M} a_i^{(2)} p_{i,1+2s}(x_{k^*}) + \sum_{r=0}^{2s} c_r^{(2)} \frac{x_{k^*}^r}{r!}, \\ &\vdots \\ y_n(x_{k^*}) &\approx \sum_{i=1}^{2M} a_i^{(n)} p_{i,1+2s}(x_{k^*}) + \sum_{r=0}^{2s} c_r^{(n)} \frac{x_{k^*}^r}{r!}. \end{aligned} \tag{11}$$

4. Convergence analysis

In this section, we discuss the two theorems associated with the convergence of both Haar wavelet based methods.

Theorem 1 (*HWCM*). *Suppose that* $\mathrm{d}^{k^*}y_p/\mathrm{d}x^{k^*}$, $k^* = 1, 2$ *and* $p = 1, 2, \ldots, n$, *exist and are bounded in* $[A, B]$. *For any* $M = 2^J$, $J = 0, 1, 2, \ldots$, *if* y_p^M *is the solution based on HWCM and* y_p *is the exact solution for each* p, *then* $\|y_p - y_p^M\|_\infty \leq \mathcal{O}\left(\frac{1}{M}\right)^2$ as $J \to \infty$.

Proof. See [31,34]. □

Theorem 2 (*H-HWCM*). *Suppose that* $\mathrm{d}^{k^*}y_p/\mathrm{d}x^{k^*}$, $k^* = 1, 2, \ldots, 2(s+1)$ *and* $p = 1, 2, \ldots, n$ *exist and are bounded in* $[A, B]$. *For any* $M = 2^J$, $J = 0, 1, 2, \ldots,$ *and* $s = 1, 2, 3, \ldots,$ *if* y_p^M *is the solution based on H-HWCM and* y_p *is the exact solution for each* p, *then* $\|y_p - y_p^M\|_\infty \le \mathcal{O}\left(\frac{1}{M}\right)^P$ as $J \to \infty$, where $P = 2 + 2s$.

Proof. First, considering $p = 1$, we have

$$E_M := \|y_1 - y_1^M\|_\infty = \max_{a\le x\le b}\left|\sum_{i=2M+1}^{\infty} a_i^{(1)} p_{i,1+2s}(x)\right|.$$

As it is assumed that $\mathrm{d}^{k+2s}y_1/\mathrm{d}x^{k+2s}$ is bounded, we have

$$E_M \le \beta \sum_{i=2M+1}^{\infty} \frac{b-a}{2^{j+1}} \max_{a\le x\le b} |p_{i,1+2s}(x)|, \tag{12}$$

where $\beta > 0$. It has been proved in [34] that $\max_{a\le x\le b} p_{i,2}(x) = \left(\frac{b-a}{2^{j+1}}\right)^2$, and following the same steps as in [34], we can easily obtain (recalling the relationship between i, k and j given in (4))

$$\max_{a\le x\le b} p_{i,1+2s}(x) \le \frac{8}{3}\frac{1}{(s_1!)^2}\left(\frac{b-a}{2^{j+1}}\right)^{2+2s}, \quad \text{for } 1+2s > 2, \tag{13}$$

where $s_1 = \lfloor \frac{1+2s}{2} \rfloor$. Using (13) in (12), we have

$$\begin{aligned}
E_M &\le \beta \sum_{j=J+1}^{\infty}\sum_{k=0}^{2^j-1}\left(\frac{b-a}{2^{j+1}}\right)\left(\frac{8}{3(s_1!)^2}\right)\left(\frac{b-a}{2^{j+1}}\right)^{2+2s}\\
&= \beta\left(\frac{8}{3(s_1!)^2}\right)\sum_{j=J+1}^{\infty}\sum_{k=0}^{2^j-1}\left(\frac{b-a}{2^{j+1}}\right)^{3+2s}\\
&= \beta\left(\frac{8(b-a)^{(3+2s)}}{3(s_1!)^2}\right)\sum_{j=J+1}^{\infty}\sum_{k=0}^{2^j-1}\left(\frac{1}{2^{j+1}}\right)^{3+2s}\\
&= \frac{\beta}{2}\left(\frac{8(b-a)^{(3+2s)}}{3(s_1!)^2}\right)\sum_{j=J+1}^{\infty}\left(\frac{1}{2^{j+1}}\right)^{2+2s}\\
&= \frac{\beta}{2^{(3+2s)}}\left(\frac{8(b-a)^{(3+2s)}}{3(s_1!)^2}\right)\sum_{j=J+1}^{\infty}\left(\frac{1}{2^{j}}\right)^{2+2s}\\
&= \frac{\beta}{2^{(3+2s)}}\left(\frac{8(b-a)^{(3+2s)}}{3(s_1!)^2}\right)\left(\frac{1}{2^{J+1}}\right)^{2+2s}\left(\frac{2^{2+2s}}{2^{2+2s}-1}\right)\\
&= \frac{8\beta(b-a)^{(3+2s)}}{6\left(2^{(2+2s)}-1\right)\left((s_1!)^2\right)}\left(\frac{1}{2^{J+1}}\right)^{2+2s} = \mathcal{O}\left(\frac{1}{M}\right)^{2+2s}.
\end{aligned}$$

The same process can be repeated for $p = 2, 3, \ldots, n$. The proof is completed. □

5. Stability analysis

To study the stability of both methods, it is essential to look at the condition number of the algebraic equations, which should be bounded [50]. For this purpose, the system of algebraic equations obtained from both Haar wavelet methods can be written as

$$H\mathcal{X} = \mathcal{B}, \tag{14}$$

where H is a matrix based on Haar functions, $\mathcal{X}$ is the unknown vector based on Haar series, and B is the right-side vector. To check the stability numerically, we use the following definition.

Table 1
The condition numbers in different cases.

J	Method	Test Problem 1	Test Problem 2	Test Problem 3	size of H
3	HWCM	1.6888E+04	6.3588E+02	7.5064E+01	34 × 34
	H-HWCM	7.7565E+07	7.9103E+04	1.5818E+04	38 × 38
4	HWCM	3.1287E+04	8.9892E+02	1.0633E+02	66 × 66
	H-HWCM	2.0140E+08	4.3105E+05	8.3301E+04	70 × 70
5	HWCM	5.3111E+04	1.2725E+03	1.5068E+02	130 × 130
	H-HWCM	4.2171E+08	2.3849E+06	4.5558E+05	134 × 134
6	HWCM	8.3716e+04	1.8012e+03	2.1338e+02	130 × 130
	H-HWCM	7.3845e+08	1.3334e+07	2.5344e+06	134 × 134
7	HWCM	1.2604e+05	2.5484e+03	3.0198e+02	258 × 258
	H-HWCM	1.2847e+09	7.4982e+07	1.4217e+07	262 × 262
8	HWCM	1.8447e+05	3.6050e+03	4.2722e+02	514 × 514
	H-HWCM	5.3949e+09	4.2289e+08	8.0089e+07	518 × 518

Definition 1 (*See [29]*)**.** Suppose a numerical method for a system of ODEs gives a sequence of matrix equations of the form $H\mathcal{X} = \mathcal{B}$. We say that the method is stable if H^{-1} exists for all sufficiently large M (for $M > M_0$, say) and if there is a constant C, independent of M, such that

$$\|H^{-1}\| \leq C \quad \text{for all} \quad M > M_0.$$

The eigenvalues of H^{-1} are simply the inverses of the eigenvalues of H (say λ), so we need to compute λ instead of the eigenvalues of H^{-1}, and they should be bounded away from zero as $M \to \infty$. So according to Definition 1, we need to compute the minimum value of $|\lambda|$ for linear and nonlinear Test Problems 1–3, which obviously represents $\rho(H^{-1})$ (see Fig. 1). We can also see from Fig. 1 that increasing M does not affect $\|H^{-1}\|_2$ to increase quickly. For linear and nonlinear ODEs, we also compare the condition number of H in Table 1, which shows that the algebraic equations of both approaches are well conditioned. Hence, both methods are numerically stable.

6. Summary of the algorithms

The algorithms of the HWCM and H-HWCM are presented as follows:

Input: $N = 2M$, $M = 2^J$, $J \in \mathbb{N} \cup \{0\}$, initial conditions.
Step 1: Compute $h_i(x)$, $p_{i,1}(x)$ and $p_{i,2}(x)$.
For $n = 1, \ldots, P$, where P is the maximum number of iteration.
Step 2: Construct $\mathcal{H}$ and B for Eq. (14) according to Section 3.1 or Section 3.2.
Step 3: Calculate the unknown Haar wavelet coefficients and integration constants using

$$\mathcal{X} = \mathcal{H}^{-1}B.$$

Step 4: Construct an approximate solution from (6) or (9).
Output: If maximum of absolute error is acceptable, then the for loop will be end; otherwise go to Step 2.

7. Numerical results

We implement both proposed methods to different types of problems to demonstrate the efficiency and applicability of our study. We have also compared the results with existing techniques in the literature. The numerical results are obtained by "MATLAB R2009b" software. The CPU time unit is considered in seconds and all the simulations are carried out on DELL PC Laptop with an Intel(R) Core(TM)i3-3110M CPU 2.40 GHz, 2 GB RAM.

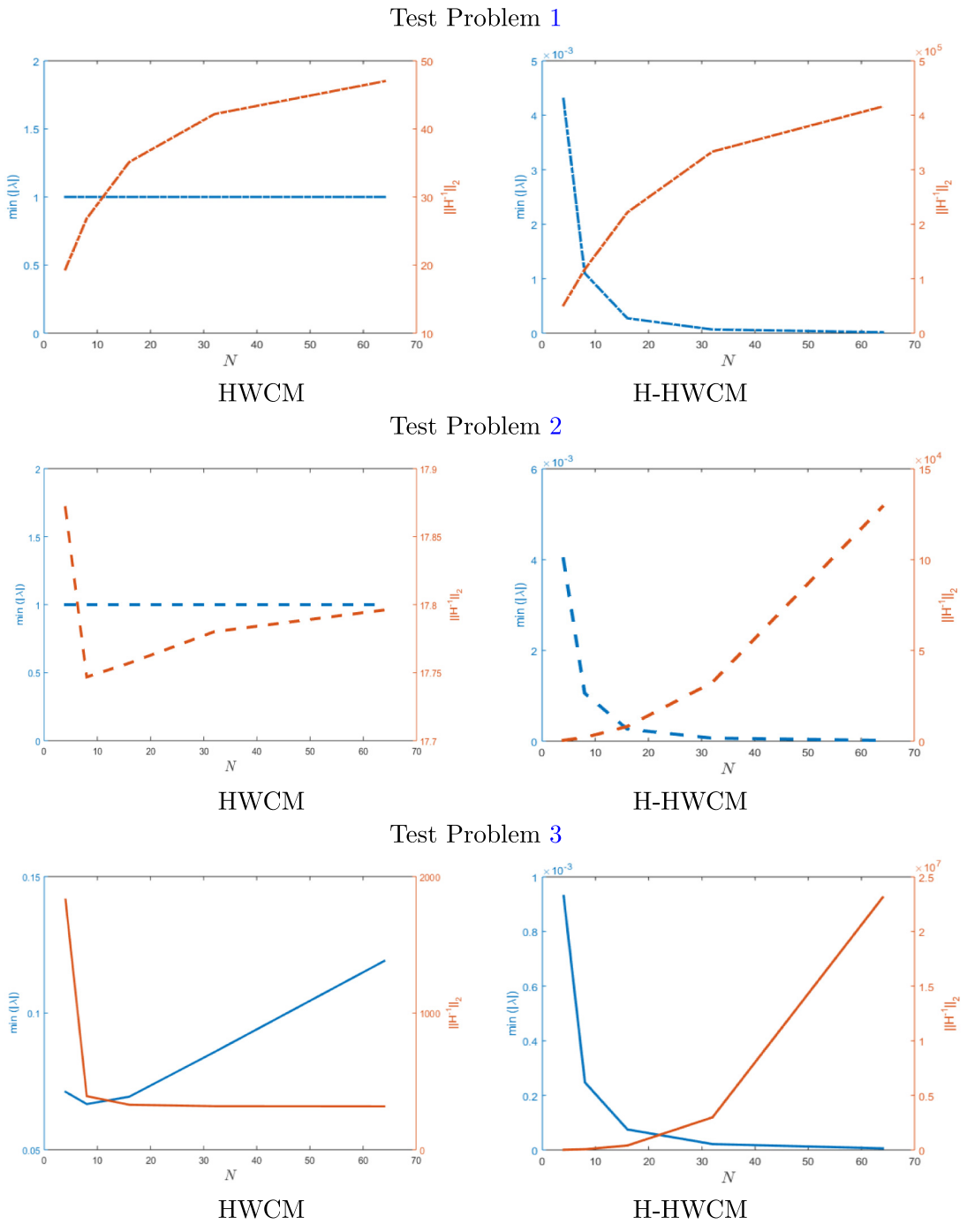

Fig. 1. $\rho(H^{-1})$ and $\|H^{-1}\|_2$.

We evaluated the effectiveness and precision of both approaches using the experimental convergence order and the L_∞ error, which are given as

$$\boldsymbol{C}_R(M) = \log\big(L_\infty(M/2)/L_\infty(M)\big)/\log(2),$$
$$L_\infty(y_p) = \max_{a\le x\le b}(|y_p(x) - y_p^M(x)|), \quad p = 1, 2, \ldots, n.$$

Table 2
Numerical results obtained by H-HWCM for Test Problem 1 (the experimental rate of convergence is in line with Theorem 2).

J	$L_\infty(y_1)$	$L_\infty(y_2)$	$C_R(y_1)$	$C_R(y_2)$	CPU time
4	5.6470E−02	5.6470E−02	–	–	0.1135
5	6.6887E−03	6.6887E−03	3.0777	3.0777	0.2918
6	5.3416e−04	5.3416e−04	3.6464	3.6464	0.8539
7	4.2096e−05	4.2096e−05	3.6655	3.6655	3.4826
8	2.9462e−06	2.9462e−06	3.8368	3.8368	13.2732

Test Problem 1. *Taking the linear stiff system*

$$\begin{aligned} \frac{\mathrm{d}y_1(x)}{\mathrm{d}x} &= -y_1(x) + 95y_2(x), \\ \frac{\mathrm{d}y_2(x)}{\mathrm{d}x} &= -y_1(x) - 97y_2(x), \end{aligned} \tag{15}$$

with given initial conditions

$$y_1(0) = 1, \quad y_2(0) = 1.$$

The exact solution is

$$y_1(x) = \frac{95e^{-2x} - 48e^{-96x}}{47}, \qquad y_2(x) = \frac{48e^{-96x} - e^{-2x}}{47}.$$

This problem has been solved by H-HWCM, and the results are compared with three different methods, namely the single-term Haar wavelet method (STHM), the classical Runge–Kutta fourth-order method (CRK), and the nonuniform Haar wavelet method (see Fig. 2), where H-HWCM and the nonuniform Haar wavelet methods are better than STHM and CRK method. In case of stiff ODEs, the nonuniform Haar wavelet method is more accurate due to considering variable stepsize (it is given in [10]), but the current study, i.e., the modification of HWCM and called as H-HWCM, is more accurate than [10]. The numerical solution of the given problem shows that H-HWCM having constant stepsize gives much more accurate results than the nonuniform Haar wavelet method and is also time efficient. The maximum error, experimental order of convergence (which is in line with Theorem 2), and the CPU time are given in Table 2 to show the performance and efficiency of the proposed H-HWCM. The comparison of numerical and exact solutions along with pointwise error obtained by H-HWCM are presented in Fig. 3.

Test Problem 2. *Consider the nonlinear system of differential equations with variable coefficients*

$$\begin{aligned} \frac{\mathrm{d}y_1(x)}{\mathrm{d}x} &= 2(y_2(x))^2, \\ \frac{\mathrm{d}y_2(x)}{\mathrm{d}x} &= e^{-x}y_1(x), \\ \frac{\mathrm{d}y_3(x)}{\mathrm{d}x} &= y_2(x) + y_3(x). \end{aligned} \tag{16}$$

The exact solution is

$$y_1(x) = e^{2x}, \quad y_2(x) = e^x, \quad y_3(x) = xe^x.$$

The initial conditions can be obtained from the exact solution. In Table 3, different methods are compared, and the pointwise error of H-HWCM is very small compared to the Adomian decomposition method (ADM) [12] and HWCM. In Table 4, the maximum error is calculated for different values of J using HWCM and H-HWCM, and it can be concluded that by increasing the values of J, the error of H-HWCM is decreasing faster than the error of HWCM, where both methods are time efficient (see the CPU time in Table 4). Comparison of the numerical solutions (H-HWCM) with the exact solution is also shown in Figs. 4–5.

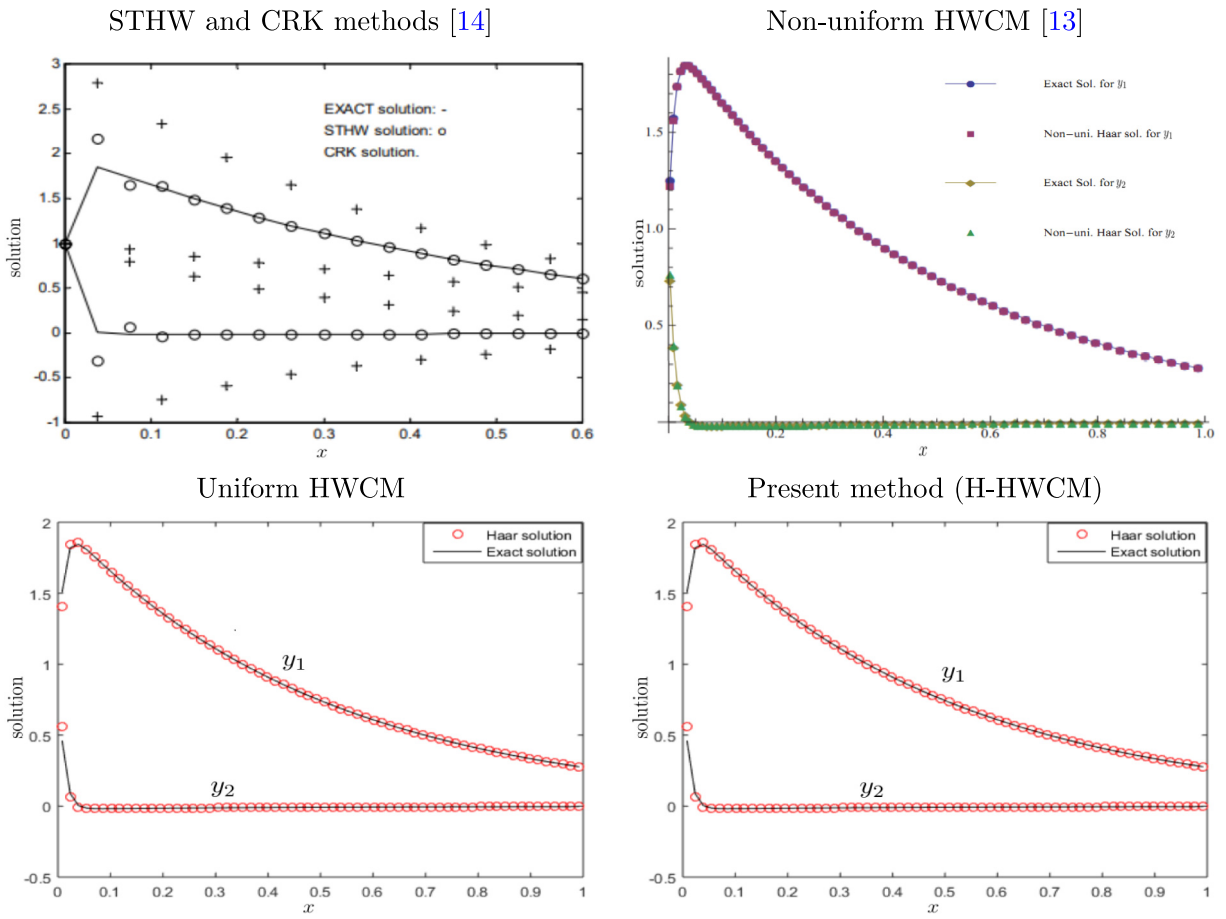

Fig. 2. Comparison of numerical solution with exact solution for Test Problem 1.

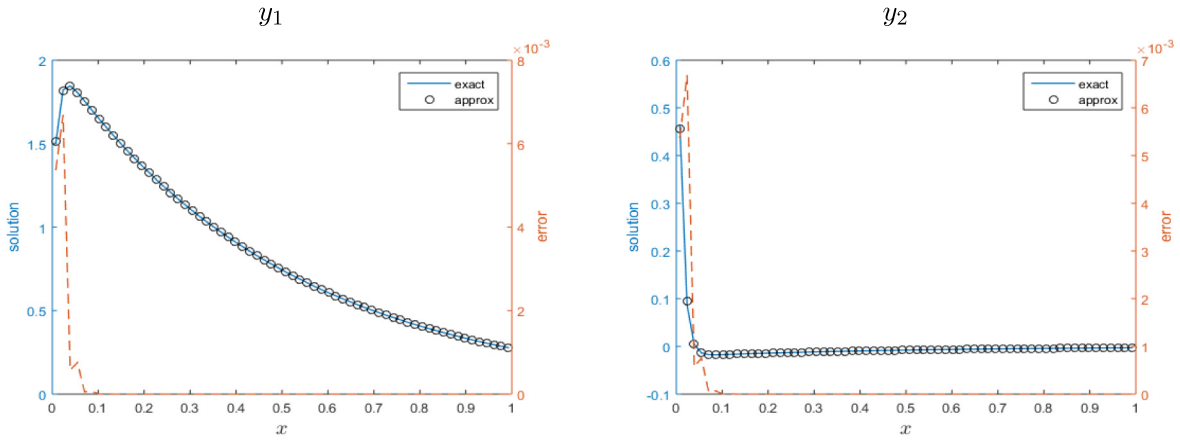

Fig. 3. Solutions and point wise error obtained by H-HWCM for Test Problem 1 at $J = 5$.

Table 3
Comparison of absolute error at various points obtained by different methods for Test Problem 2.

x	ADM [12]			HWCM ($J = 5$)			H-HWCM ($s = 1$, $J = 5$)		
	y_1	y_2	y_3	y_1	y_2	y_3	y_1	y_2	y_3
0.1	1.653E−5	2.932E−6	0	1.504E−4	4.446E−5	7.557E−5	3.386E−9	4.518E−10	8.199E−10
0.2	5.337E−5	1.121E−5	0	1.372E−4	4.999E−5	7.031E−5	2.947E−9	7.590E−10	7.410E−10
0.3	5.974E−4	1.140E−4	5.116E−5	1.891E−4	6.956E−5	9.340E−5	4.650E−9	1.265E−9	1.139E−9
0.4	3.131E−3	5.729E−4	2.732E−4	3.445E−4	1.071E−4	1.563E−4	9.653E−9	2.017E−9	2.167E−9
0.5	1.134E−2	1.959E−3	9.885E−4	1.417E−4	8.808E−5	7.653E−5	7.177E−9	2.584E−9	1.851E−9
0.6	3.206E−2	5.249E−3	2.807E−3	6.152E−4	1.713E−4	2.475E−4	1.842E−8	3.811E−9	3.861E−9
0.7	7.666E−2	1.190E−2	6.760E−3	6.591E−4	1.932E−4	2.548E−4	1.978E−8	4.861E−9	4.293E−9
0.8	1.625E−1	2.392E−2	1.144E−2	9.006E−4	2.412E−4	3.223E−4	2.773E−8	6.327E−9	5.719E−9
0.9	3.144E−1	4.384E−2	2.796E−2	1.450E−3	3.222E−4	4.725E−4	4.217E−8	8.243E−9	8.431E−9

Table 4
Comparison of HWCM and H-HWCM for Test Problem 2.

J	HWCM				H-HWCM ($s = 1$)			
	$L_\infty(y_1)$	$L_\infty(y_2)$	$L_\infty(y_3)$	CPU time	$L_\infty(y_1)$	$L_\infty(y_2)$	$L_\infty(y_3)$	CPU time
2	1.07E−01	2.28E−02	3.37E−02	0.0128	9.65E−04	3.46E−05	3.68E−05	0.0657
3	2.89E−02	5.99E−03	8.91E−03	0.0464	5.68E−04	4.53E−06	2.48E−06	0.0955
4	7.52E−03	1.54E−03	2.29E−03	0.0480	2.90E−04	1.58E−06	1.62E−07	0.1094
5	1.92E−03	3.90E−04	5.82E−04	0.1838	1.45E−04	4.25E−07	1.12E−08	0.3169
6	4.85E−04	9.83E−05	1.46E−04	0.5164	7.26E−05	1.08E−07	7.78E−10	1.0809
7	1.22E−04	2.46E−05	3.68E−05	0.9139	3.63E−05	2.71E−08	5.62E−11	1.7129
8	3.05E−05	6.18E−06	9.22E−06	1.4315	1.81E−06	6.79E−09	4.40E−12	2.4371

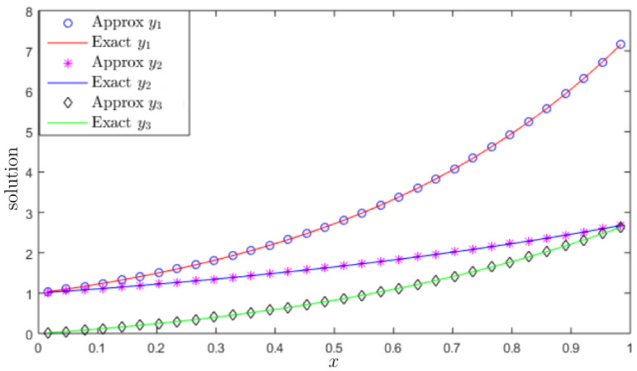

Fig. 4. Comparison of H-HWCM results with exact solution at $s = 1$ and $J = 4$ for Test Problem 2.

Test Problem 3. *Consider the system of highly nonlinear and nonhomogeneous differential equations [27]*

$$\begin{aligned} \frac{\mathrm{d}y_1(x)}{\mathrm{d}x} &= \cos(x) + (y_1(x))^2 + y_2(x) - (1 + x^2 + \sin^2(x)), \\ \frac{\mathrm{d}y_2(x)}{\mathrm{d}x} &= 2x - (1 + x^2)\sin(x) + y_1(x)y_2(x), \end{aligned} \tag{17}$$

with initial conditions $y_1(0) = 0$ *and* $y_2(0) = 1$. *The exact solution is*

$$y_1(x) = \sin(x), \qquad y_2(x) = 1 + x^2.$$

We have compared the results obtained by different techniques in the interior points of the interval $[0, 2]$ *in Table 5 and also highlighted the absolute errors at* $x_i \in [0, 2]$ *of these different methods. The maximum error and CPU times are compared in Table 6, and the accuracy of H-HWCM is better than HWCM, but in terms of time efficiency*

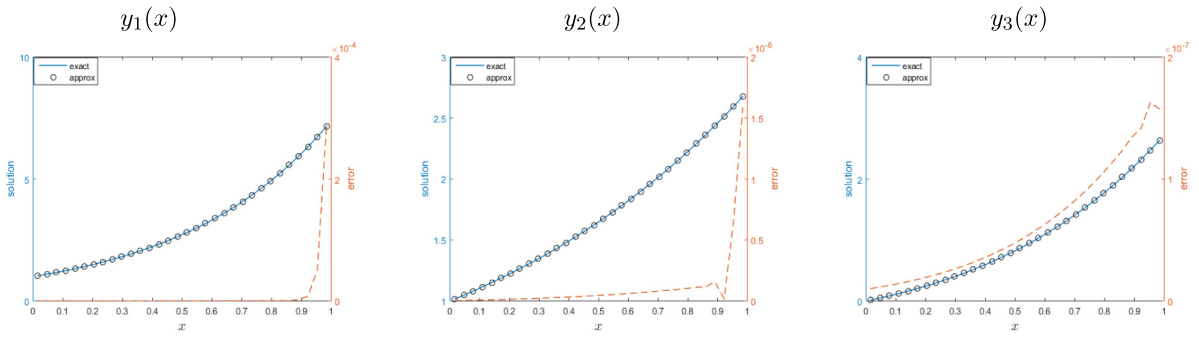

Fig. 5. Comparison of H-HWCM results with exact solution at $s = 1$ and $J = 5$ for Test Problem 2.

Table 5
Comparison of numerical results obtained by different methods for Test Problem 3.

x		0.1	0.3	0.6	0.9	1.2	1.5	1.8
LeNN [37]	$y_1(x)$	0.0995	0.2970	0.5679	0.7833	0.9327	0.9974	0.9800
	$y_2(x)$	0.9862	1.0908	1.3687	1.8106	2.4418	3.2498	4.2402
MLP [37]	$y_1(x)$	0.1019	0.2998	0.5689	0.7864	0.9329	0.9949	0.9810
	$y_2(x)$	1.0030	1.0973	1.3628	1.8056	2.4383	2.2542	4.2468
HWCM	$y_1(x)$	0.0999	0.2957	0.5652	0.7847	0.9357	1.0071	0.9993
	$y_2(x)$	1.0109	1.0907	1.3613	1.8121	2.4441	3.2607	4.2763
H-HWCM	$y_1(x)$	0.0998	0.2955	0.5646	0.7833	0.9320	0.9974	0.9737
	$y_2(x)$	1.0100	1.0900	1.3600	1.8100	2.4400	3.2501	4.2402
Exact	$y_1(x)$	0.0998	0.2955	0.5646	0.7833	0.9320	0.9975	0.9738
	$y_2(x)$	1.0100	1.0900	1.3600	1.8100	2.4400	3.2500	4.2400
Absolute error of LeNN	$y_1(x)$	3.00E−3	5.07E−3	5.84E−3	0.0000	7.51E−4	1.00E−4	6.36E−3
	$y_2(x)$	2.35E−2	7.33E−4	6.39E−3	3.31E−4	7.37E−4	6.15E−5	4.97E−5
Absolute error of MLP	$y_1(x)$	2.10E−2	1.45E−2	7.61E−3	3.95E−3	9.65E−4	2.60E−3	7.39E−3
	$y_2(x)$	6.93E−3	6.69E−3	2.05E−3	2.43E−3	6.96E−4	1.29E−3	1.60E−3
Absolute error of HWCM	$y_1(x)$	1.00E−3	6.76E−4	1.06E−3	1.78E−3	3.96E−3	9.62E−3	2.61E−2
	$y_2(x)$	8.91E−4	6.42E−4	9.55E−4	1.16E−3	1.68E−3	3.29E−3	8.65E−3
Absolute error of H-HWCM	$y_1(x)$	2.75E−10	2.19E−10	3.81E−10	6.77E−10	2.87E−10	5.03E−10	8.48E−10
	$y_2(x)$	1.35E−12	1.29E−11	5.53E−11	1.04E−10	6.13E−12	7.19E−12	7.94E−12

Table 6
Comparison of HWCM with H-HWCM ($s = 1$) for Test Problem 3.

J	HWCM		CPU time	H-HWCM		CPU time
	$L_\infty(y_1)$	$L_\infty(y_2)$		$L_\infty(y_1)$	$L_\infty(y_2)$	
3	1.7431E−03	2.4924E−03	0.0301	1.6904E−04	1.0579E−05	0.0704
4	4.5390E−04	6.4206E−04	0.1091	8.0472E−05	2.5718E−06	0.1477
5	1.1598E−04	1.6315E−04	0.2385	3.9270E−05	6.3332E−07	0.3183
6	2.9324E−05	4.1138E−05	0.5114	1.9399E−05	1.5708E−07	0.9574

there is no such big difference in the performance of both methods. The comparison of different methods with the exact solution in the interval $[0, 2]$ *is also shown in Fig. 6.*

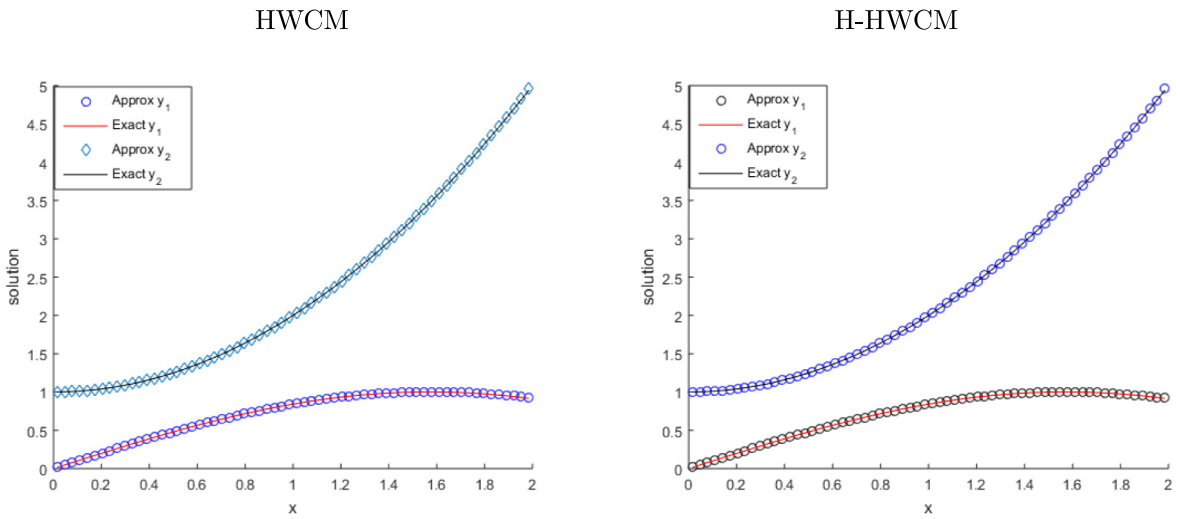

Fig. 6. Comparison of results obtained by HWCM and H-HWCM at $J = 5$ with exact solution for Test Problem 3.

Test Problem 4. *Consider the system of nonlinear differential equations for an infectious disease, where t is the independent variable instead of x*

$$\begin{aligned}
\frac{\mathrm{d}S}{\mathrm{d}t} &= a - \frac{\beta SI}{N} - \mu S,\\
\frac{\mathrm{d}E_1}{\mathrm{d}t} &= q\frac{\beta SI}{N} - (\mu + \varepsilon_1)E_1 + (1-\eta)\delta T,\\
\frac{\mathrm{d}E_2}{\mathrm{d}t} &= (1-q)\frac{\beta SI}{N} + \varepsilon_1 E_1 - (\mu + \varepsilon_2)E_2,\\
\frac{\mathrm{d}I}{\mathrm{d}t} &= \varepsilon_2 E_2 + \eta\delta T - (\mu + \gamma + \sigma_1)I,\\
\frac{\mathrm{d}T}{\mathrm{d}t} &= \gamma I - (\mu + \delta + \sigma_2 + \alpha)T,\\
\frac{\mathrm{d}R}{\mathrm{d}t} &= \alpha T - \mu R,
\end{aligned} \tag{18}$$

subject to the initial conditions

$$S(0) = 30, \quad E_1(0) = 80, \quad E_2(0) = 50, \quad I(0) = 80, \quad T(0) = 5, \quad R(0) = 5. \tag{19}$$

In (18), we assume

$$N(t) = S(t) + E_1(t) + E_2(t) + I(t) + T(t) + R(t), \tag{20}$$

where $N(t)$ is the total population including the susceptible class $S(t)$, slow exposed class $E_1(t)$, fast exposed class $E_2(t)$, infected class $I(t)$, class with proper treatment $T(t)$, and recovered individuals $R(t)$. The parameters in (18) are defined in Table 7.

The exact solution of this problem is not given, so we have compared our results with the results reported in [24], where the same behaviors of the solutions are clearly visible in Fig. 7. We have also showed the behavior of solutions after different years in Fig. 8. Based on the performance of the proposed method observed in the above problems, we can conclude that the results obtained in this case are also accurate.

The minimum value of $|\lambda|$ is calculated in this case as well, which obviously represents the magnitude of $\rho(H^{-1})$ (see Fig. 9). From Fig. 9, it is also clear that increasing M does not affect $\|H^{-1}\|_2$ to increase quickly, which means that H^{-1} exists and is bounded, and hence this is a sufficient condition for stability of the numerical results.

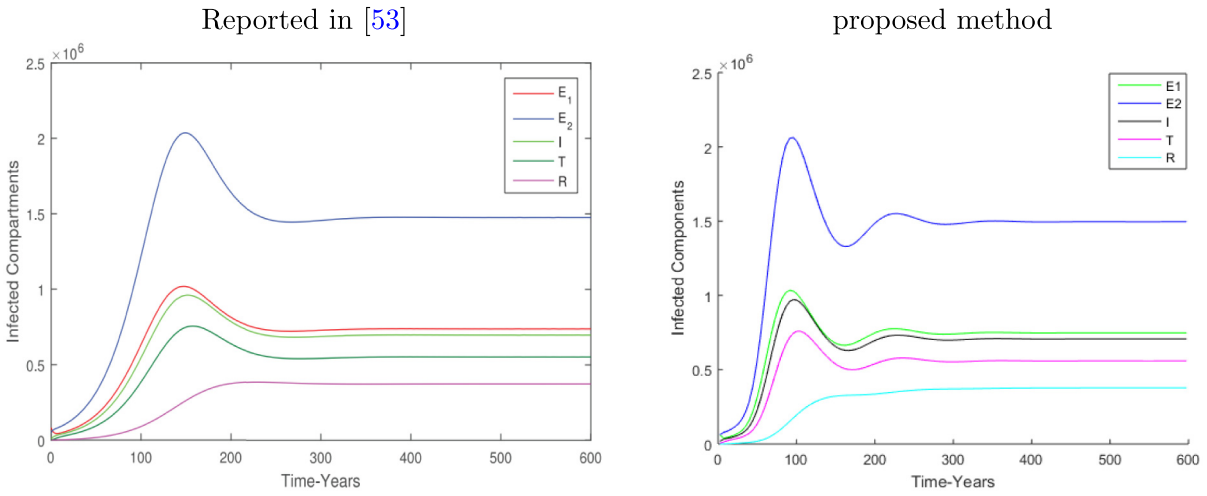

Fig. 7. Comparison of numerical solution obtained by different methods for Test Problem 4.

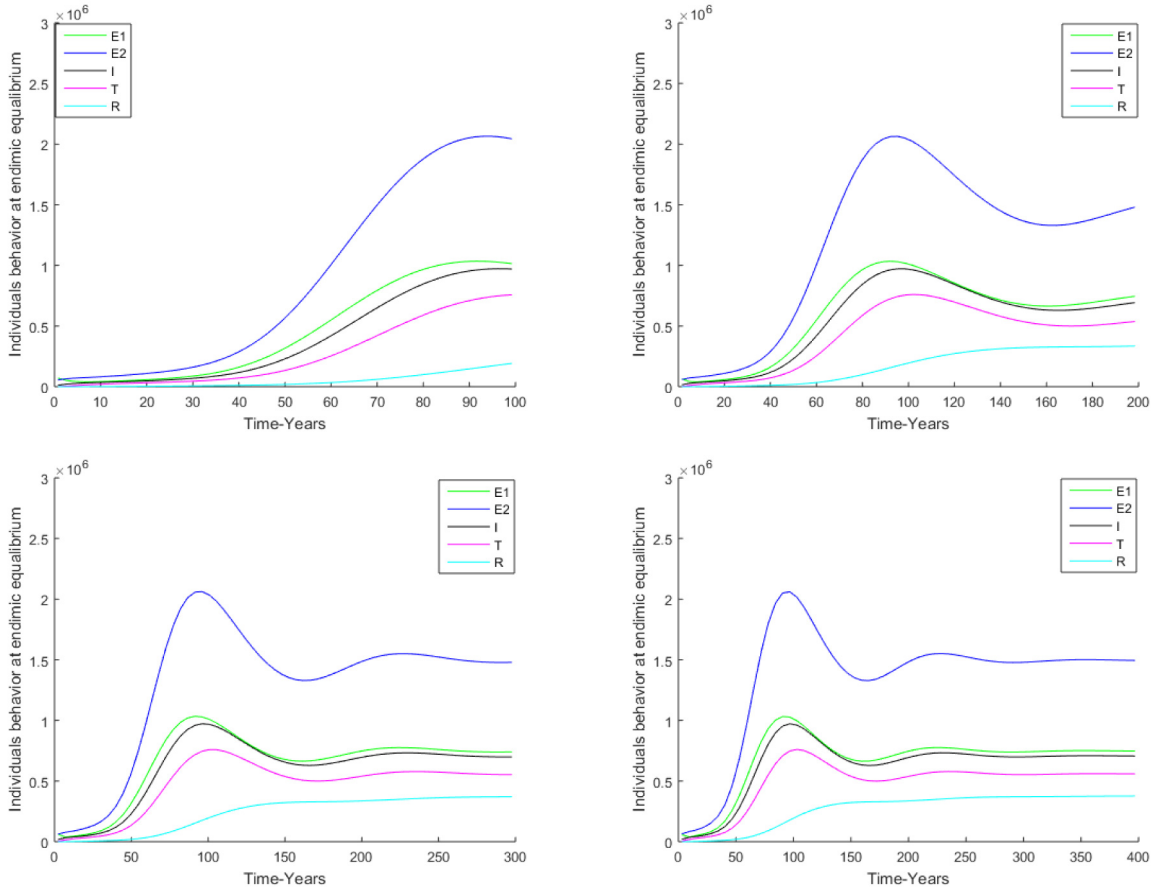

Fig. 8. The behaviors of the numerical results after various years for Test Problem 4.

Table 7
Estimated or fitted values of parameters for Test Problem 4.

Parameter	Detail	Baseline value
a	Birth rate	450,862.20088
β	Contact rate	0.6001
α	Recovery rate	0.01
γ	Treatment rate of infective individuals	0.1500
μ	Natural mortality rate	1/67.7
σ_1	Disease induced death rate in I	0.2738
σ_2	Disease induced death rate during treatment	0.1000
δ	Leaving rate of treated individual re-enter to I or E1	0.0649
η	Failure of treatment	0.2959
ε_1	Rate of moving from E1 to E2	0.2351
ε_2	Transfer rate from E2 to I	0.2001
q	Fraction of susceptible individuals being infected	0.5259

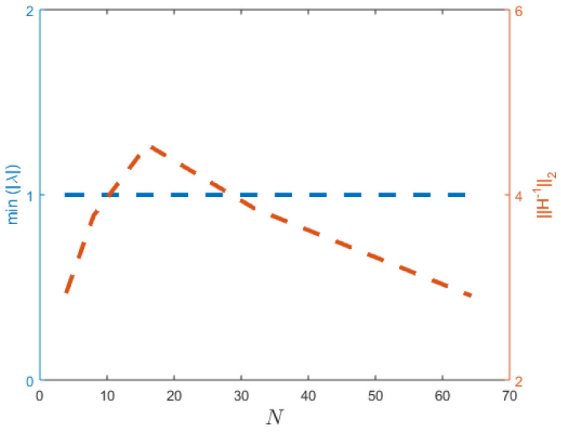

Fig. 9. $\rho(H^{-1})$ and $\|H^{-1}\|_2$ for Test Problem 4.

8. Conclusion

In this article, HWCM and H-HWCM are used to solve systems of linear and nonlinear ordinary differential equations in combination with the quasi-linearization technique. The numerical results are stable, time efficient, and in line with theoretical orders of convergence. Both methods are effective and provide accurate and acceptable results, but it is clear from the tables that H-HWCM is more accurate and of faster convergence than HWCM. The current approaches can be extended to PDEs and systems of PDEs with some modifications. This is the focus of our future projects.

Acknowledgment

The second author would like to acknowledge the financial supports from the research grant JCYJ 20210324121402008 by Shenzhen Science and Technology Innovation Commission.

References

[1] M. Ahsan, I. Ahmad, M. Ahmad, I. Hussain, A numerical Haar wavelet-finite difference hybrid method for linear and non-linear Schrödinger equation, Math. Comput. Simulation 165 (2019) 13–25, http://dx.doi.org/10.1016/j.matcom.2019.02.011.

[2] M. Ahsan, M. Ahmad, W. Khan, E.E. Mahmoud, A.-H. Abdel-Aty, Meshless analysis of nonlocal boundary value problems in anisotropic and inhomogeneous media, Mathematics 8 (11) (2020) 2045.

[3] M. Ahsan, M. Bohner, A. Ullah, A.A. Khan, S. Ahmad, A Haar wavelet multi-resolution collocation method for singularly perturbed differential equations with integral boundary conditions, Math. Comput. Simulation 204 (2023) 166–180, http://dx.doi.org/10.1016/j.matcom.2022.08.004.

[4] M. Ahsan, I. Hussain, M. Ahmad, A finite-difference and Haar wavelets hybrid collocation technique for non-linear inverse Cauchy problems, Appl. Math. Sci. Eng. 30 (1) (2022) 121–140, http://dx.doi.org/10.1080/17415977.2022.2026350.
[5] M. Ahsan, W. Lei, A.A. Khan, A. Ullah, S. Ahmad, S.U. Arifeen, Z. Uddin, H. Qu, A high-order reliable and efficient Haar wavelet collocation method for nonlinear problems with two point-integral boundary conditions, Alex. Eng. J. 71 (2023) 185–200.
[6] M. Ahsan, S. Lin, M. Ahmad, M. Nisar, I. Ahmad, H. Ahmed, X. Liu, A Haar wavelet-based scheme for finding the control parameter in nonlinear inverse heat conduction equation, Open Phys. 19 (1) (2021) 722–734, http://dx.doi.org/10.1515/phys-2021-0080.
[7] M. Ahsan, K. Shams-ul-Haq, X. Liu, S. Ahmad, M. Nisar, A Haar wavelets based approximation for nonlinear inverse problems influenced by unknown heat source, Math. Methods Appl. Sci. (2022) 1–13.
[8] M. Ahsan, Siraj-ul-Islam, I. Hussain, Haar wavelets multi-resolution collocation analysis of unsteady inverse heat problems, Inverse Problems in Science and Engineering 27 (11) (2018) 1498–1520, http://dx.doi.org/10.1080/17415977.2018.1481405.
[9] M. Ahsan, T. Tran, Siraj-ul-Islam, I. Hussain, A multiresolution collocation method and its convergence for Burgers' type equations, Math. Methods Appl. Sci. (2022) 1–24.
[10] I. Aziz, Y. Shumaila, T. Pavel, Numerical solution of stiff ODEs using non-uniform Haar wavelets, AIP Conf. Proc. 2116 (1) (2019) 330008, http://dx.doi.org/10.1063/1.5114346.
[11] I. Aziz, Siraj-ul-Islam, F. Khan, A new method based on Haar wavelet for the numerical solution of two-dimensional nonlinear integral equations, J. Comput. Appl. Math. 272 (2014) 70–80, http://dx.doi.org/10.1016/j.cam.2014.04.027.
[12] J. Biazar, E. Babolian, R. Islam, Solution of the system of ordinary differential equations by Adomian decomposition method, Appl. Math. Comput. 147 (3) (2004) 713–719, http://dx.doi.org/10.1016/S0096-3003(02)00806-8.
[13] C. Chen, C. Hsiao, Haar wavelet method for solving lumped and distributed-parameter systems, IEEE Proc. D 144 (1) (1997) 87–94.
[14] J. Douglas Jr., B.F. Jones Jr., On predictor-corrector methods for nonlinear parabolic differential equations, J. Soc. Ind. Appl. Math. 11 (1963) 195–204.
[15] Z.-J. Fu, S. Reutskiy, H.-G. Sun, J. Ma, M.A. Khan, A robust kernel-based solver for variable-order time fractional PDEs under 2D/3D irregular domains, Appl. Math. Lett. 94 (2019) 105–111, http://dx.doi.org/10.1016/j.aml.2019.02.025.
[16] Z. Fu, Z. Tang, Q. Xi, Q. Liu, Y. Gu, F. Wang, Localized collocation schemes and their applications, Acta Mech. Sin. 38 (7) (2022) 422167, http://dx.doi.org/10.1007/s10409-022-22167-x, pp. 28.
[17] C. Guo, J. Hu, J. Hao, S. Celikovsky, X. Hu, Fixed-time safe tracking control of uncertain high-order nonlinear pure-feedback systems via unified transformation functions, 59, (3) 2023, pp. 342–364, arXiv preprint arXiv:2305.00505.
[18] G. Hariharan, Haar wavelet method for solving the Klein–Gordon and the sine-Gordon equations, Int. J. Nonlinear Sci. 11 (2) (2011) 180–189.
[19] G. Hariharan, K. Kannan, Haar wavelet method for solving Cahn–Allen equation, Appl. Math. Sci. (Ruse) 3 (49–52) (2009) 2523–2533.
[20] C.-H. Hsiao, State analysis of linear time delayed systems via Haar wavelets, Math. Comput. Simulation 44 (5) (1997) 457–470, http://dx.doi.org/10.1016/S0378-4754(97)00075-X.
[21] C.-H. Hsiao, Haar wavelet approach to linear stiff systems, Math. Comput. Simulation 64 (5) (2004) 561–567, http://dx.doi.org/10.1016/j.matcom.2003.11.011.
[22] C.-H. Hsiao, W.-J. Wang, Haar wavelet approach to nonlinear stiff systems, Math. Comput. Simul. 57 (6) (2001) 347–353.
[23] H.-Y. Jin, Z.-A. Wang, Boundedness, blowup and critical mass phenomenon in competing chemotaxis, J. Differential Equations 260 (1) (2016) 162–196.
[24] M.A. Khan, M. Ahmad, S. Ullah, M. Farooq, T. Gul, Modeling the transmission dynamics of tuberculosis in Khyber Pakhtunkhwa Pakistan, Adv. Mech. Eng. 11 (6) (2019) 1–13, http://dx.doi.org/10.1177/1687814019854835.
[25] E. Kreyszig, Advanced Engineering Mathematics, tenth ed., John Wiley & Sons, Inc., New York, 2020, pp. xvi+1156+A97+I20.
[26] A. Kurnaz, G. Oturanç, The differential transform approximation for the system of ordinary differential equations, Int. J. Comput. Math. 82 (6) (2005) 709–719, http://dx.doi.org/10.1080/00207160512331329050.
[27] I.E. Lagaris, A. Likas, D.I. Fotiadis, Artificial neural networks for solving ordinary and partial differential equations, IEEE Trans. Neural Netw. 9 (5) (1998) 987–1000.
[28] Ü. Lepik, Numerical solution of evolution equations by the Haar wavelet method, Appl. Math. Comput. 185 (1) (2007) 695–704, http://dx.doi.org/10.1016/j.amc.2006.07.077.
[29] R.J. LeVeque, Finite Difference Methods for Ordinary and Partial Differential Equations, Society for Industrial and Applied Mathematics (SIAM), Philadelphia, PA, 2007, p. xvi+341, http://dx.doi.org/10.1137/1.9780898717839.
[30] X. Liu, M. Ahsan, M. Ahmad, I. Hussain, M.M. Alqarni, E.E. Mahoud, Haar wavelets multi-resolution collocation procedures for two-dimensional nonlinear Schrödinger equation, Alex. Eng. J. 60 (3) (2021) 3057–3071, http://dx.doi.org/10.1016/j.aej.2021.01.033, URL: https://www.sciencedirect.com/science/article/pii/S1110016821000387.
[31] X. Liu, M. Ahsan, M. Ahmad, M. Nisar, X. Liu, I. Ahmad, H. Ahmad, Applications of Haar wavelet-finite difference hybrid method and its convergence for hyperbolic nonlinear Schrödinger equation with energy and mass conversion, Energies 14 (23) (2021) 7831, pp. 17.
[32] J. Majak, M. Pholak, K. Karjust, M. Eerme, J. Kurnitski, B. Shvartsman, New higher order Haar wavelet method: Application to FGM structures, Compos. Struct. 201 (2018) 72–78, http://dx.doi.org/10.1016/j.compstruct.2018.06.013.
[33] J. Majak, M. Pohlak, M. Eerme, B. Shvartsman, Solving ordinary differential equations with higher-order Haar wavelet method, AIP Conf. Proc. 2116 (1) (2019) 330002, http://dx.doi.org/10.1063/1.5114340.
[34] J. Majak, B. Shvartsman, M. Kirs, M. Pohlak, H. Herranen, Convergence theorem for the Haar wavelet based discretization method, Compos. Struct. 126 (2015) 227–232.
[35] J. Majak, B. Shvartsman, M. Pohlak, K. Karjust, M. Eerme, E. Tungel, Solution of fractional order differential equation by the Haar wavelet method. Numerical convergence analysis for most commonly used approach, AIP Conf. Proc. 1738 (1) (2016) 480110, http://dx.doi.org/10.1063/1.4952346.

[36] J. Majak, B. Shvartsman, M. Ratas, D. Bassir, M. Pohlak, K. Karjust, M. Eerme, Higher-order Haar wavelet method for vibration analysis of nanobeams, Mater. Today Commun. 25 (2020) 101290.
[37] S. Mall, S. Chakraverty, Application of Legendre neural network for solving ordinary differential equations, Appl. Soft Comput. 43 (5) (2016) 347–356, http://dx.doi.org/10.1016/j.asoc.2015.10.069.
[38] M. Mehrparvar, J. Majak, K. Karjust, M. Arda, Free vibration analysis of tapered Timoshenko beam with higher order Haar wavelet method, Proc. Est. Acad. Sci. 71 (1) (2022) 77–83.
[39] Q. Meng, Q. Ma, Y. Shi, Adaptive fixed-time stabilization for a class of uncertain nonlinear systems, IEEE Trans. Automat. Control (2023) 1–8., http://dx.doi.org/10.1109/TAC.2023.3244151.
[40] M. Mikola, J. Majak, M. Pohlak, B. Shvartsman, Higher order Haar wavelet method for vibration analysis of functionally graded beam, AIP Conf. Proc. 2425 (1) (2022).
[41] S. Nazir, S. Shahzad, R. Wirza, R. Amin, M. Ahsan, N. Mukhtar, I. García-Magariño, J. Lloret, Birthmark based identification of software piracy using Haar wavelet, Math. Comput. Simulation 166 (2019) 144–154, http://dx.doi.org/10.1016/j.matcom.2019.04.010.
[42] R. Norberg, Differential equations for moments of present values in life insurance, Insurance Math. Econom. 17 (2) (1995) 171–180, http://dx.doi.org/10.1016/0167-6687(95)00019-O.
[43] Y. Pinchover, J. Rubinstein, An Introduction to Partial Differential Equations, Cambridge University Press, Cambridge, 2005, p. xii+371, http://dx.doi.org/10.1017/CBO9780511801228.
[44] M. Ratas, A. Salupere, Application of higher order Haar wavelet method for solving nonlinear evolution equations, Math. Model. Anal. 25 (2) (2020) 271–288, http://dx.doi.org/10.3846/mma.2020.11112.
[45] J.N. Reddy, Introduction to the Finite Element Method, fourth ed., McGraw-Hill Education, New York, 2019.
[46] S. Reutskiy, Z.-J. Fu, A semi-analytic method for fractional-order ordinary differential equations: Testing results, Fract. Calc. Appl. Anal. 21 (6) (2018) 1598–1618, http://dx.doi.org/10.1515/fca-2018-0084.
[47] H.J. Ricardo, A Modern Introduction to Differential Equations, third ed., Academic Press, 2020.
[48] Siraj-ul-Islam, M. Ahsan, I. Hussain, A multi-resolution collocation procedure for time-dependent inverse heat problems, Int. J. Therm. Sci. 128 (2018) 160–174, http://dx.doi.org/10.1016/j.ijthermalsci.2018.01.001, URL: https://www.sciencedirect.com/science/article/pii/S1290072917301011.
[49] M. Sorrenti, M. Di Sciuva, J. Majak, F. Auriemma, Static response and buckling loads of multilayered composite beams using the refined zigzag theory and higher-order Haar wavelet method, Mech. Compos. Mater. 57 (2021) 1–18.
[50] H. Sun, L. Mei, Y. Lin, A new algorithm based on improved Legendre orthonormal basis for solving second-order BVPs, Appl. Math. Lett. 112 (2021) 1–9, Paper No. 106732, http://dx.doi.org/10.1016/j.aml.2020.106732.
[51] A. Wambecq, Rational Runge-Kutta methods for solving systems of ordinary differential equations, Computing 20 (4) (1978) 333–342, http://dx.doi.org/10.1007/BF02252381.
[52] M. Zhong, Q.-J. Yang, S.-F. Tian, The modified high-order Haar wavelet scheme with Runge–Kutta method in the generalized Burgers–Fisher equation and the generalized Burgers–Huxley equation, Modern Phys. Lett. B 35 (24) (2021) 2150419, http://dx.doi.org/10.1142/S0217984921504194, pp. 16.
[53] D.G. Zill, Introduction to the Finite Element Method, ninth ed., Cengage Learning, Boston, 2018.